Astron. Astrophys. 334, 153–158 (1998)

ASTRONOMY
AND
ASTROPHYSICS

Correlated nucleosynthesis of fluorine and s-process elements in asymptotic giant branch stars

N. Mowlavi[1], **A. Jorissen**[2⋆], **and M. Arnould**[2]

[1] Observatoire de Genève, CH-1290 Sauverny, Switzerland
[2] Institut d'Astronomie et d'Astrophysique, Université Libre de Bruxelles, C.P.226, Boulevard du Triomphe, B-1050 Brüssel, Belgium

Received 24 September 1997 / Accepted 2 January 1998

Abstract. The production of fluorine and s-process elements in conditions simulating the helium-burning shell of asymptotic giant branch (AGB) stars is investigated from parametric one-zone nucleosynthesis calculations. Our calculations account for the correlation between the overabundances of these elements, as observed at the surface of S and C stars (Jorissen et al. 1992, A&A 261, 164). A primary supply of ^{13}C is, however, required to produce ^{19}F and s-process elements at the observed levels through the operation of the ^{13}C(α,n)^{16}O neutron source. Our calculations allow to put strong constraints on this primary supply. They require a ^{13}C mass fraction of at least 0.003, with little sensitivity to the stellar conditions. This value is about 30 times larger than the secondary ^{13}C supply available at the end of the CNO cycle in solar-metallicity stars. The minimum ^{14}N mass fractions required are found to vary between about $6\ 10^{-4}$ and 0.01, depending on the temperature at which the fluorine production occurs.

Key words: nucleosynthesis – stars: abundances – stars: AGB

1. Introduction

The discovery by Jorissen et al. (1992; hereafter JSL) that fluorine is overabundant at the surface of S and C stars has provided a definite proof that these stars can be net producers of ^{19}F. A reaction path to produce ^{19}F in a helium-burning environment had already been proposed by Goriely et al. (1989), provided that protons are available. Fluorine then results from $^{14}\mathrm{N}\,(\alpha\,,\gamma)\,^{18}\mathrm{F}\,(\beta^{+})\,^{18}\mathrm{O}\,(\mathrm{p}\,,\alpha)\ \ ^{15}\mathrm{N}\,(\alpha\,,\gamma)\,^{19}\mathrm{F}$. The necessary protons may be produced by (n,p) reactions, whereas ^{14}N is always abundant at the onset of He burning, since basically all CNO nuclei are transformed into ^{14}N during the former operation of the CNO cycle. Such conditions are met in the helium-burning shell (HeBS) of asymptotic giant branch (AGB) stars, where the necessary protons are released by $^{14}\mathrm{N}\,(\mathrm{n}\,,\mathrm{p})\,^{14}\mathrm{C}$, with neutrons from $^{13}\mathrm{C}\,(\alpha\,,\mathrm{n})\,^{16}\mathrm{O}$. Detailed AGB model calculations have confirmed such a scenario for ^{19}F production (Mowlavi et al. 1996, hereafter MJA; see also Forestini et al. 1992). They have shown that fluorine is produced either in the radiative layers of the HeBS, or in the convective 'thermal pulses' which develop recurrently in the HeBS of AGB stars as a result of thermal instabilities. However, the MJA model predictions for the ^{19}F yields are unable to account for the overabundances observed at the surface of AGB stars. A way to reconcile the model predictions with the observations is to increase the neutron fluences in the AGB models. In the MJA models, only the 'secondary' ^{13}C supply left behind by the hydrogen-burning shell (HBS) is available for neutron production. That supply is in fact limited by the initial CNO abundances in the HBS (which in turn depend on the star's metallicity). Clearly, if neutrons are to be released by $^{13}\mathrm{C}\,(\alpha\,,\mathrm{n})\,^{16}\mathrm{O}$, a larger ^{13}C supply is needed to produce ^{19}F at the observed levels. Primary ^{13}C might in fact be produced following the mixing of protons with ^{12}C from the HeBS, the abundance of which is metallicity- independent (Jorissen & Arnould 1989; Herwig et al. 1997).

This need for a primary source of ^{13}C leading to large neutron fluences in the HeBS of AGB stars parallels a similar requirement for activating the s-process in these stars. The s-process is a chain of neutron captures producing nuclides along the valley of nuclear stability. Heavy elements primarily produced by the s-process are overabundant at the surface of AGB stars, as demonstrated by spectroscopic analyses of S stars (Smith & Lambert 1990). The s-process has even operated recently in these stars, as assessed by the detection of Tc whose isotope 99 is produced by the s-process (Little et al. 1987). Although the need for a primary ^{13}C supply in AGB stars has already been expressed about 20 years ago, it has never been obtained in a fully self-consistent way in models of low-mass, solar-metallicity stars (see the discussion about the 's-process mystery' by Sackmann & Boothroyd 1991). Progress in that direction has been reported recently, however (Herwig et al. 1997).

In any case, the conditions prevailing during the operation of the s-process are expected to lead as well to the production of large amounts of ^{19}F. The correlated production of ^{19}F and s-process elements, first suggested by Jorissen & Arnould (1989) and Goriely et al. (1989), is actually supported by the observations of AGB stars, which show that all ^{19}F-rich stars are also enriched in s-process elements (see Fig. 12 of JSL).

Send offprint requests to: N. Mowlavi
⋆ Research Associate, National Fund for Scientific Research (FNRS), Belgium

The efficiency of ^{19}F production, i.e., the ratio of ^{19}F nuclei produced to the number of available neutrons, has been shown by MJA to depend on various physical and chemical parameters characterizing the HeBS, such as temperature, rate of ^{13}C injection into the pulse, or abundance of ^{26}Al left behind by the HBS. It is the purpose of this paper to analyse the fluorine production in an environment with neutron fluences large enough for allowing the s-process operation. Because AGB models currently fail to provide such an environment in a self-consistent way, we base our analysis on one-zone parametric nucleosynthesis calculations, with constant temperature and density, and with the initial ^{13}C and ^{14}N abundances taken as free parameters. These calculations thus allow us to investigate the consequences of radiative ^{13}C burning during the interpulse phase. Convective ^{13}C burning in the thermal pulse would require a more sophisticated treatment involving mass-averaged reaction rates over the convective zone, which is model-dependent and will not be considered in this paper. The present one-zone calculations are nevertheless relevant, since recent AGB calculations indicate that, if primary ^{13}C fuel is present, it should mainly burn radiatively during the interpulse phase (Straniero et al. 1995; Herwig et al. 1997).

The adopted initial abundances and nuclear-reaction network are described in Sect. 2. The results of our computations are used to draw the flow chart of combined ^{19}F and s-process syntheses in Sect. 3. The sensitivity of the ^{19}F and s-process yields to the initial ^{13}C and ^{14}N supplies, as well as to temperature, is described in Sect. 4. Sect. 5 confronts the results with the observations. Conclusions are drawn in Sect. 6.

2. Initial conditions, nuclear network and typical results

Primary ^{13}C is produced when protons from the H-rich envelope are mixed in the ^{12}C-rich layers left behind by the convective pulse (Jorissen & Arnould 1989; Herwig et al. 1997). The partial operation of the CN cycle then leads to the production of the required ^{13}C nuclei. In this process, primary ^{14}N is also produced, adding to any pre-existing supply. The initial mass fractions of ^{13}C and ^{14}N are thus taken as free parameters, ranging from 10^{-4} to $5\ 10^{-2}$. For comparison, the equilibrium operation of the CNO cycle in the HBS of solar-metallicity AGB stars leads to $X(^{13}\mathrm{C}) \sim 10^{-4}$ and $X(^{14}\mathrm{N}) \sim 1.5\ 10^{-2}$ (MJA).

In a first set of calculations, no ^{19}F is assumed to be present initially in order to analyse its net production from the initial ^{13}C and ^{14}N supplies. The efficiency of the ^{19}F production may then be evaluated from

$$g_{\rm eff} = X(^{19}\mathrm{F}) \ / \ \frac{19}{13} X_0(^{13}\mathrm{C}), \qquad (1)$$

where $X_0(^{13}\mathrm{C})$ is the initial ^{13}C supply, and $X(^{19}\mathrm{F})$ the final ^{19}F mass fraction. The above definition implicitely assumes that the considered timescale is long enough for $^{15}\mathrm{N}\,(\alpha\,,\gamma)\,^{19}\mathrm{F}$ to have converted into ^{19}F all the ^{15}N produced in the process. Moreover, ^{15}N and ^{18}O, both directly involved in the chain producing ^{19}F (see Sect. 1), have negligible initial abundances (see below), so that they ought not be included in $g_{\rm eff}$ (see MJA for more details).

As noted by MJA, $^{19}\mathrm{F}\,(\mathrm{n}\,,\gamma)\,^{20}\mathrm{F}$ may lead to a substantial ^{19}F destruction in s-process environments. This destruction only affects the ^{19}F that is initially present, however. This results from the slow ^{19}F synthesis by $^{15}\mathrm{N}\,(\alpha\,,\gamma)\,^{19}\mathrm{F}$ relative to the much faster $^{13}\mathrm{C}\,(\alpha\,,\mathrm{n})\,^{16}\mathrm{O}$ neutron production. In order to evaluate the level of ^{19}F destruction by neutron captures, we have thus performed additional calculations with $X_0(^{19}\mathrm{F}) = 10^{-4}$, i.e. about 250 times solar. This concentration may result from ^{19}F production episodes earlier in the AGB evolution.

The initial abundances of all the other elements from H to S are taken from a detailed AGB model of a $3\ \mathrm{M}_\odot$ solar-metallicity star (Mowlavi 1995). These abundances are typical of those characterising the outer layers of the ^{12}C-rich zone left behind by a thermal pulse. The initial abundances of elements heavier than sulfur are solar. Most of these abundances have no impact on the outcome of the nucleosynthesis process under consideration. The only initial abundances that need to be mentioned because of their possible relevance are $X_0(^{15}\mathrm{N}) = 4\ 10^{-6}$ and $X_0(^{18}\mathrm{O}) = 7.4\ 10^{-7}$ (involved in the ^{19}F production chain; see Sect. 1), $X_0(^{20}\mathrm{Ne}) = 1.6\ 10^{-3}$ (which acts as a proton poison; see Fig. 1), and $X_0(^{26}\mathrm{Al}) = 1\ 10^{-5}$ [which may possibly act as a proton source through $^{26}\mathrm{Al}\,(\mathrm{n}\,,\mathrm{p})\,^{26}\mathrm{Mg}$]. In the present calculations, the adopted initial ^{15}N, ^{18}O and ^{26}Al abundances are too small to have any impact on the outcome of the process (but see MJA for a discussion of specific situations – like early thermal pulses or more massive AGB stars – where this is no more the case).

The nuclear network used in our computations includes 472 nuclei (from neutrons and protons to ^{210}Po) linked by 834 reactions. Reactions involving nuclei up to ^{28}Si are those listed in Jorissen & Arnould (1989). They include all proton-, neutron- and α-captures relevant up to $T_8 = 3$ (T_8 refers to the temperature expressed in units of 10^8 K). For nuclei heavier than ^{34}S, only radiative neutron captures and β-decays are considered, plus a few (n,p) and (n,α) reactions. Our neutron-capture network is able to handle neutron densities up to about 10^{13} neutrons cm^{-3}. Cross sections are taken from Caughlan & Fowler (1988) (for reactions involving charged particles) or from Beer et al. (1992) (for neutron-capture reactions), except when more recent determinations are available (as listed in the Appendix of MJA). The equations describing the evolution of the abundances are linearized according to Wagoner's (1969) prescription, and the resulting set of algebraic equations is solved as described in Appendix B of Prantzos et al. (1987).

The s-process efficiency is evaluated from the number

$$N_{\rm c} = \sum_{A=57}^{209} 56\ (A-56)\ [X(A) - X_0(A)]\ /\ [A\ X_0(^{56}\mathrm{Fe})] \qquad (2)$$

of neutrons captured per initial ^{56}Fe nucleus, where $X(A)$ stands for the mass fraction of the nuclides with atomic mass A.

Several calculations have been performed to investigate how the efficiency of ^{19}F and s-process production, expressed in terms of $g_{\rm eff}$ and N_c, depends on $X_0(^{13}\mathrm{C})$ and $X_0(^{14}\mathrm{N})$, as well on temperature.

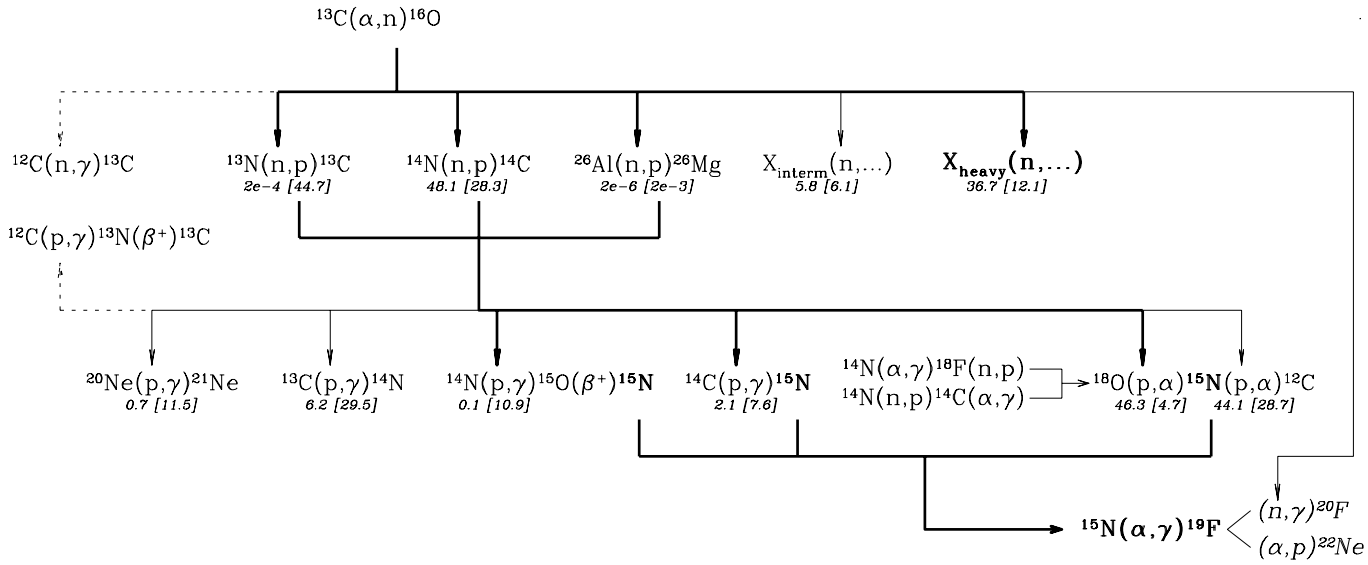

Fig. 1. The reaction chain involved in the production of ^{19}F and s-process elements in the neutron-rich environment of the He-burning shell in AGB stars. The path leading to these elements is indicated by thick lines. Reactions destroying ^{19}F are written in italics. $X_{\rm interm}(n,...)$ and $X_{\rm heavy}(n,...)$ represent the neutron-capture reactions by the intermediate-mass nuclei (Si to Mn), and by Fe and heavier nuclei, respectively. Dotted lines represent reactions involving n- and p-captures which eventually replenish ^{13}C, and are consequently not real 'poison' reactions. The numbers below the n-capture (respectively p-capture) reactions illustrate their relative importance, in % of the total flux of n-capture (respectively p-capture) reactions, when $T_8 = 1$ (2 for numbers in brackets), $\rho = 4000$ g/cm^3, and $X_0(^{13}\mathrm{C})$=$X_0(^{14}\mathrm{N})$=10^{-2}. We stress that *these numbers depend sensitively upon the adopted conditions*. Only reactions contributing more than 3% (at either temperature) have been represented, with the exception of $^{26}\mathrm{Al}\,(\mathrm{n}\,,\mathrm{p})\,^{26}\mathrm{Mg}$, since this reaction may be an important proton source if ^{26}Al were more abundant initially (see text)

A first set of calculations is performed at $T_8 = 1$. This value is close to the temperatures characterizing radiative ^{13}C burning in the intershell region (Straniero et al. 1995). Test calculations reveal that the conclusions are about identical for all relevant temperatures up to about $T_8 = 1.7$. At higher temperatures, however, a 'hot' mode of fluorine production sets in where the nuclear flows are quite different from the 'cold' mode at $T_8 \lesssim 1.7$. A second set of calculations is thus performed at $T_8 = 2$. If some ^{13}C survives radiative burning and is ingested in the convective pulse, the resulting nucleosynthesis should be close to this situation.

Contours of equal $g_{\rm eff}$ and N_c values in the [$X_0(^{13}\mathrm{C})$, $X_0(^{14}\mathrm{N})$] plane will be presented in Sect. 4 for $T_8 = 1$ and 2. As a first step, however, the flow chart of combined ^{19}F and s-process synthesis is drawn in Sect. 3.

3. The nuclear transformations governing the ^{19}F production in neutron-rich He-burning layers

The reaction chain producing both ^{19}F and elements heavier than iron in neutron-rich He-burning layers of AGB stars has been summarized in Fig. 1 of MJA. When the neutron fluence is high enough for an efficient s-process nucleosynthesis, the nuclear reaction chain leading to ^{19}F becomes more intricate, however, as shown in Fig. 1.

The main features of the combined fluorine and s-process nucleosynthesis may be summarized as follows:

(1) the s-process nucleosynthesis operates directly from the neutrons released by $^{13}\mathrm{C}\,(\alpha\,,\mathrm{n})\,^{16}\mathrm{O}$. In contrast, the ^{19}F production requires another seed (^{14}N) in order to operate. In fact, ^{14}N plays a double role in the ^{19}F synthesis: it is the starting point of the reaction chain leading to ^{19}F and it provides, through ^{14}N(n,p)^{14}C, the necessary protons involved in that chain;

(2) ^{14}N and the heavy nuclei (i.e. ^{56}Fe and heavier) are the dominant neutron captors, their relative contribution depending on their respective abundances. Therefore, the relative efficiency of the ^{19}F and s-process syntheses depends on the ^{14}N abundance, large values favouring ^{19}F. Conversely, large ^{13}C initial abundances favour the s-process synthesis. Indeed, the associated large neutron fluences substantially destroy ^{14}N through $^{14}\mathrm{N}\,(\mathrm{n}\,,\mathrm{p})\,^{14}\mathrm{C}$. For large ^{13}C supplies, the s-process is thus comparatively more efficient than the ^{19}F synthesis;

(3) the role played by ^{13}N deserves a special attention. At temperatures $T_8 \sim 2$ ('hot' mode of F production), the neutron and ^{13}N abundances resulting from $^{13}\mathrm{C}\,(\alpha\,,\mathrm{n})\,^{16}\mathrm{O}$ and $^{12}\mathrm{C}\,(\mathrm{p}\,,\gamma)\,^{13}\mathrm{N}$ are large enough in order for $^{13}\mathrm{N}\,(\mathrm{n}\,,\mathrm{p})\,^{13}\mathrm{C}$ to be the dominant neutron captor, and to be faster than ^{13}N(β^+)^{13}C. In those conditions, $^{12}\mathrm{C}\,(\mathrm{p}\,,\gamma)\,^{13}\mathrm{N}\ (\mathrm{n}\,,\mathrm{p})\,^{13}\mathrm{C}\ (\alpha\,,\mathrm{n})\,^{16}\mathrm{O}$ sets in, and recycles both neutrons and protons. Fluorine and s-process syntheses are possible only from the protons and neutrons leaking out of this recycling process. This situation makes the nucleosynthesis quite intricate. In particular, the ^{19}F yield in that regime is almost independent of the initial ^{13}C supply (see Fig. 3);

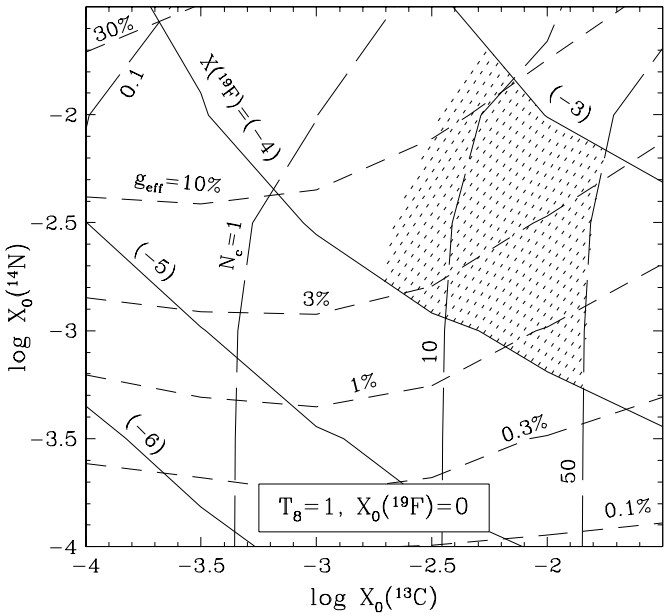

Fig. 2. Contours of several quantities at the end of ^{13}C burning as a function of $X_0(^{13}\mathrm{C})$ and $X_0(^{14}\mathrm{N})$ at $T_8 = 1$ and $\rho = 4000$ g cm^{-3}: the final fluorine mass fraction [$X(^{19}\mathrm{F})$, solid lines], the efficiency of its production ($g_{\rm eff}$, short-dashed lines), and the number of neutrons captured per ^{56}Fe nucleus (N_c, long-dashed lines). Numbers in parentheses refer to powers of ten. The hatched region outlines the constraints on $X_0(^{13}\mathrm{C})$ and $X_0(^{14}\mathrm{N})$ set by the observed values of N_c and $X(^{19}\mathrm{F})$ (see text)

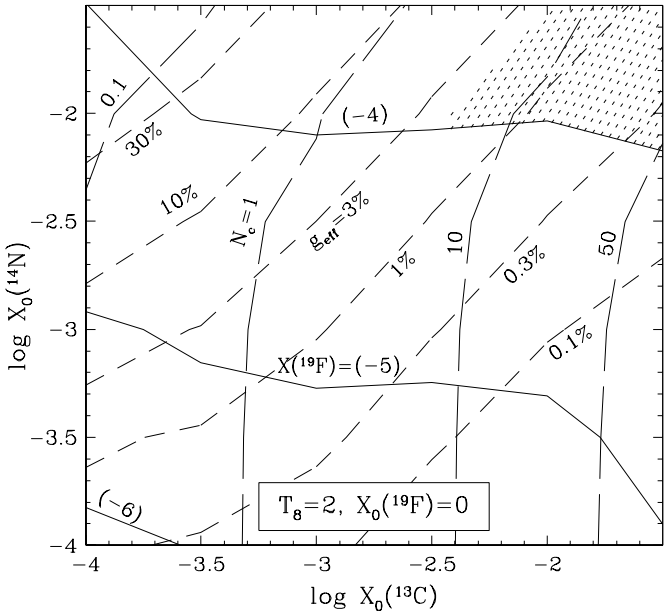

Fig. 3. Same as Fig. 2, but at $T_8 = 2$ and $\rho = 4000$ g cm^{-3}

(4) Up to 45% of the protons made available through (n,p) reactions are captured by ^{15}N, and constitute the main loss of efficiency during fluorine production;

(5) The $^{19}\mathrm{F}\,(\mathrm{n}\,,\gamma)\,^{20}\mathrm{F}$ reaction does lead to a substantial destruction of ^{19}F in s-process environments (see Figs. 4 and 5).

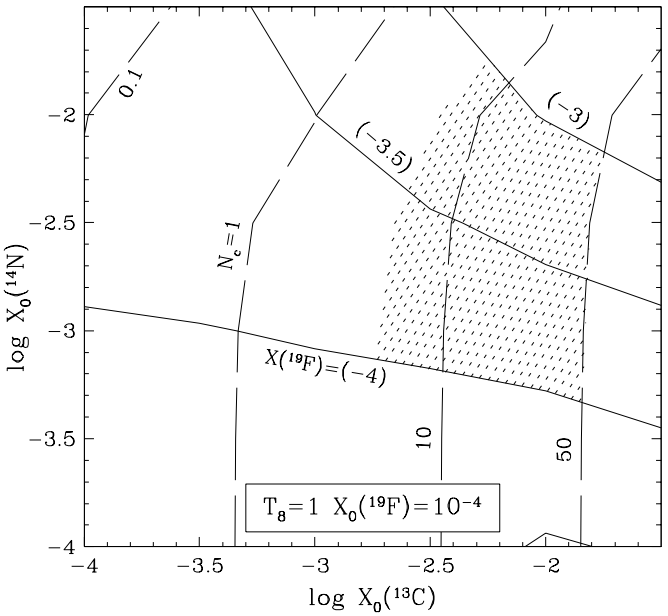

Fig. 4. Same as Fig. 2 for $X_0(^{19}\mathrm{F}) = 10^{-4}$. For clarity, contours of $g_{\rm eff}$ are not presented

4. Charts of ^{19}F and s-process yields

The values of $X(^{19}\mathrm{F})$, $g_{\rm eff}$ and $N_{\rm c}$ at the end of ^{13}C burning are displayed in Figs. 2 ($T_8 = 1$) and 3 ($T_8 = 2$), as a function of the initial ^{13}C and ^{14}N supplies.

At $T_8 = 1$, the final fluorine abundances depend with an almost equal sensitivity on both the initial ^{13}C and ^{14}N abundances (see Sect. 3): lines of constant $X(^{19}\mathrm{F})$ in Fig. 2 almost coincide with lines of constant $\log X_0(^{13}\mathrm{C}) + \log X_0(^{14}\mathrm{N})$. At $T_8 = 2$, the ^{19}F yield becomes almost independent of the initial ^{13}C abundance, because the process is now controlled by $^{12}\mathrm{C}\,(\mathrm{p}\,,\gamma)\,^{13}\mathrm{N}\,(\mathrm{n,p})\,^{13}\mathrm{C}\,(\alpha\,,\mathrm{n})\,^{16}\mathrm{O}$. This chain recycles ^{13}C, neutrons and protons, so that the production of ^{19}F only depends on the fraction of protons and neutrons leaking out of this main chain. The ^{19}F yields are thus quite temperature-dependent, and this dependence is mainly caused by the switch between different regimes of neutron and proton balance occurring at the temperature where $^{13}\mathrm{N}\,(\mathrm{n}\,,\mathrm{p})\,^{13}\mathrm{C}$ becomes faster than $^{13}\mathrm{N}(\beta^+)^{13}\mathrm{C}$.

In contrast, the s-process yields are almost independent of temperature. Comparing contours of N_c at $T_8 = 1$ and 2 (Figs. 2 and 3), there is only a slight loss of efficiency as the temperature increases. Another difference between fluorine production and s-process is the weak sensitivity of the latter to the initial ^{14}N supply, at least for $X_0(^{14}\mathrm{N}) \lesssim 5\ 10^{-3}$. For higher $X_0(^{14}\mathrm{N})$ values, however, $^{14}\mathrm{N}\,(\mathrm{n}\,,\mathrm{p})\,^{14}\mathrm{C}$ becomes a strong neutron poison which reduces the number of neutrons available for captures by the heavy elements, and the s-process efficiency is reduced accordingly. The same conclusions hold true at both $T_8 = 1$ and 2.

The impact of $^{19}\mathrm{F}\,(\mathrm{n}\,,\gamma)\,^{20}\mathrm{F}$ may be evaluated by comparing Fig. 2 with Fig. 4, and Fig. 3 with Fig. 5. The importance of $^{19}\mathrm{F}\,(\mathrm{n}\,,\gamma)\,^{20}\mathrm{F}$ is best assessed by remarking that the

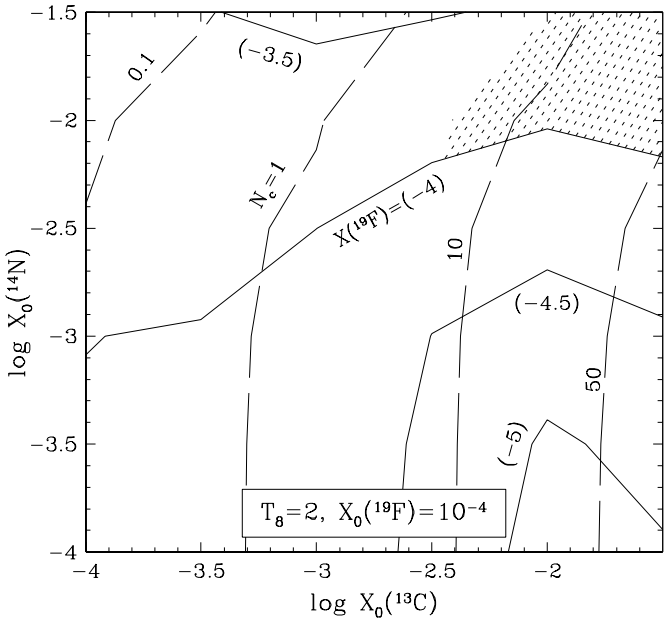

Fig. 5. Same as Fig. 3 for $X_0(^{19}\mathrm{F}) = 10^{-4}$. For clarity, contours of $g_{\rm eff}$ are not presented

final $X(^{19}\mathrm{F})$ abundance is, in a large region of the $[X_0(^{13}\mathrm{C}), X_0(^{14}\mathrm{N})]$ plane, *smaller* than the initial $X_0(^{19}\mathrm{F}) = 10^{-4}$ abundance, indicating that the initial ^{19}F has been destroyed. As expected, this destruction is largest in the region of largest N_c.

5. Implications for AGB models

By confronting the results obtained in Sect. 4 with observed abundances of ^{19}F and s-process elements at the surface of S and C stars, it is possible to constrain to some extent the primary ^{13}C and ^{14}N abundances required in AGB stars.

Observations of s-process elements in AGB stars require neutron exposures ranging from 0.2 to 1.0 mbarn^{-1} (Busso et al. 1995), which translates into $N_c \sim 5$ to 50, according to Fig. 9 of Jorissen & Arnould (1989). According to Figs. 2–5, this requires *a primary* $X(^{13}\mathrm{C})$ *supply of at least* $3\ 10^{-3}$, with no strong constraints neither on $X(^{14}\mathrm{N})$, nor on the temperature (compare Figs. 2 and 3).

Observations of fluorine abundances at the surface of red giants, on the other hand, require intershell ^{19}F abundances of the order 10^{-4} to 10^{-3} (Fig. 9 of JSL). The region of the $[X_0(^{13}\mathrm{C}), X_0(^{14}\mathrm{N})]$ plane satisfying these constraints on N_c and $X(^{19}\mathrm{F})$ has been hatched in Figs. 2–5. *A minimum* $X_0(^{14}\mathrm{N})$ *supply of* $6\ 10^{-4}$ *appears to be required* (Fig. 2). That value increases up to 10^{-2} if the ^{19}F nucleosynthesis operates at $T_8 = 2$ (Fig. 3).

Such values for $X_0(^{14}\mathrm{N})$ are naturally reached in the ashes of the H-burning shell of AGB stars, so that no further primary ^{14}N supply is actually needed. The required minimum value for $X_0(^{13}\mathrm{C})$, however, is about 30 times higher than that left over by the H-burning shell, and thus calls for an additional source of ^{13}C. Such ^{13}C abundances are, however, not unexpected if its primary production were to result from the mixing of protons into carbon-rich layers (see e.g. Table 7 of Jorissen & Arnould 1989).

6. Conclusions

The present parametric one-zone calculations confirm that the production of fluorine and s-process elements are correlated, as suggested by the abundances observed at the surface of S and C stars (Jorissen et al. 1992). More specifically, the present calculations show that

- the s-process efficiency depends mainly on the initial ^{13}C abundance, and very little on ^{14}N. Its sensitivity to ^{14}N increases, however, with temperature, in such a way that the s-process is less efficient for larger ^{14}N supplies;

- the fluorine production, on the other hand, depends on both the initial ^{13}C and ^{14}N abundances, increasing with larger $X_0(^{13}\mathrm{C})$ or $X_0(^{14}\mathrm{N})$ supplies at $T_8 = 1$. At $T_8 = 2$, however, the ^{19}F production becomes almost independent of the initial ^{13}C abundance.

The confrontation of our results with observed abundances of fluorine and s-process elements at the surface of red giant stars sets constraints on the abundances of primary ^{13}C and ^{14}N produced by AGB stars. The primary ^{13}C mass fraction must be at least equal to $3\ 10^{-3}$, this value being quite insensitive to the stellar conditions. The ^{14}N mass fraction, on the other hand, has to amount at least to $6\ 10^{-4}$ if the fluorine production operates at $T_8 = 1$, and to 10^{-2} at $T_8 = 2$. These ^{14}N abundances are in fact naturally reached in the ashes of the HBS in AGB stars, so that no further primary ^{14}N supply is actually needed. Clearly, the next step in this field is to obtain the required primary ^{13}C supply self-consistently in complete AGB models.

Acknowledgements. This work is supported in part by the *Fonds National de la Recherche Scientifique* of Belgium and in part by that of Switzerland.

References

Beer H., Voss F., Winters R.R., 1992, ApJS 80, 403
Busso M., Lambert D.L., Beglio L., Gallino R., Raiteri C.M., Smith V.V., 1995, ApJ 446, 775
Caughlan, G.R., Fowler, W.A., 1988, Atomic Data and Nucl. Data Tables 40, 283
Forestini M., Goriely S., Jorissen A., Arnould M., 1992, A&A 261, 157
Goriely S., Jorissen A., Arnould M., 1989, in Hillebrandt W., Müller E, (eds) Proc. 5th Workshop on Nuclear Astrophys., Ed. (Max Planck Inst. für Astrophys. Rep.), p60
Herwig F., Blöcker T., Schönberner D., El Eid M., 1997, A&A 324, L81
Jorissen A., Arnould M., 1989, A&A 221, 161
Jorissen A., Smith V.V., Lambert D.L., 1992, A&A 261, 164 (JSL)
Little S.J., Little-Marenin I.R., Hagen Bauer W., 1987, AJ 94, 981
Mowlavi N., 1995 *Ph. D. Thesis*, Université Libre de Bruxelles, Belgium (unpublished)
Mowlavi N., Jorissen A., Arnould M., 1996, A&A 311, 803 (MJA)
Prantzos N., Arnould M., Arcoragi J.P., 1987, ApJ 315, 209

Sackmann I.-J., Boothroyd A.I., 1991. In: Michaud G., Tutukov A. (eds.) Evolution of Stars: The Photospheric Abundance Connection (IAU Symp. 145). Kluwer, Dordrecht, p. 275
Smith V.V., Lambert D.L., 1990, ApJS 72, 387
Straniero O., Gallino R., Busso M., Chieffi A., Raiteri C.M., Limongi M., Salaris M., 1995, ApJ 440, L85
Wagoner R.W., 1969, ApJS 18, 247